

**UNCLASSIFIED**

---

---

**AD 248 599**

*Reproduced  
by the*

**ARMED SERVICES TECHNICAL INFORMATION AGENCY  
ARLINGTON HALL STATION  
ARLINGTON 12, VIRGINIA**



---

---

**UNCLASSIFIED**

NOTICE: When government or other drawings, specifications or other data are used for any purpose other than in connection with a definitely related government procurement operation, the U. S. Government thereby incurs no responsibility, nor any obligation whatsoever; and the fact that the Government may have formulated, furnished, or in any way supplied the said drawings, specifications, or other data is not to be regarded by implication or otherwise as in any manner licensing the holder or any other person or corporation, or conveying any rights or permission to manufacture, use or sell any patented invention that may in any way be related thereto.

S - 27  
Copy No. 63-A  
Dec. 23, 1960

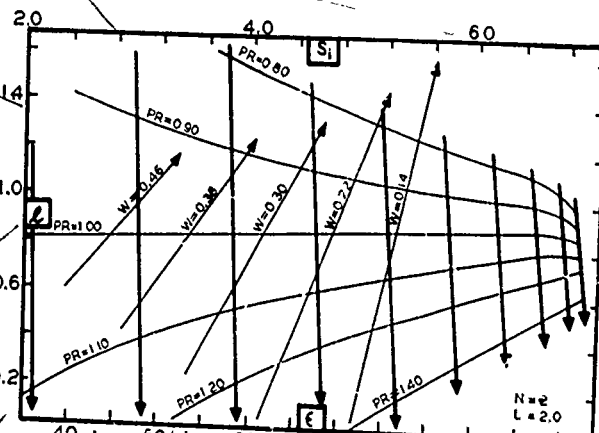
ROHM & HAAS COMPANY  
REDSTONE ARSENAL RESEARCH DIVISION  
HUNTSVILLE, ALABAMA

ASTIA  
CATALOGED BY  
AS AD NO.

2448 599

THE SHOTTED TUBE  
GRAIN DESIGN

61-1-S-  
XEROX



ASTIA

REF ID: A

JAN 9 1961

NIPUR

# ROHM & HAAS COMPANY

REDSTONE ARSENAL RESEARCH DIVISION  
HUNTSVILLE, ALABAMA

REPORT NO. S-27

## THE SLOTTED-TUBE GRAIN DESIGN

By

Max W. Stone

Approved:

*Henry M. Shuey*  
H. M. Shuey, Head  
Ballistics Section

*Allen R. Deschere*  
Allen R. Deschere  
General Manager

December 23, 1960

Work reported herein was carried  
out under contract number  
DA-01-021 ORD-11878

# ROHM & HAAS COMPANY

REDSTONE ARSENAL RESEARCH DIVISION  
HUNTSVILLE, ALABAMA

## ABSTRACT

A mathematical analysis was made of the internal-burning slotted-tube configuration, which has some distinct advantages for certain solid propellant applications. Those advantages are zero sliver, high loading density and thick web capability, low stress concentration, and mandrels that can be made cheaply and in a relatively short time. The disadvantage centers in the fact that an insulating liner is required to protect the motor wall in the slot region.

The results of the mathematical analysis were programmed for an electronic computer and calculations made for a wide range of the parameters of interest. These data have been prepared in graphical form for greater utility.

## THE SLOTTED-TUBE GRAIN DESIGN

### INTRODUCTION

ever increasing demand for missiles with greater thrust capability has caused rocket designers to investigate all means of improving the efficiency of rockets. The desirability of higher impulse propellants and of lighter and stronger metal parts has received due emphasis. In recent years the design of solid propellant grain configurations has taken on new meaning with the requirement that the greatest efficiency be realized in every phase of rocket performance. The technical literature has recorded this increased interest in an activity that was for a time classed as an art rather than a science. A recent survey paper<sup>1</sup> on grain design contains a large list of such papers. The time has just about passed when a grain designer must know from experience and memory, or evolve by trial and error with compass and straight edge, the configuration which most nearly meets the particular requirements at hand.

The present paper is a continuation of grain design work in which Rohm & Haas has been interested since 1954. Previously published work<sup>2</sup> has centered around the star, wagon wheel, and modified wagon wheel designs.

<sup>1</sup>J. A. Vandenkerckhove, "Recent Advances in Solid Propellant Grain Design", ARS Journal, 29, No. 7, 483 (1959)

<sup>2</sup>Rohm & Haas Company, Quarterly Progress Report on Interior Ballistics, No. P-55-15, August 1955(Confidential). This report contains description, equations, and design graphs for the star design.

Rohm & Haas Company Quarterly Progress Report on Interior Ballistics, No. P-56-1, February 1956 (Confidential). This report contains description, equations, and design graphs for the wagon wheel (HR) design.

Max W. Stone, "A Practical Mathematical Approach to Grain Design", Jet Propulsion, 28 No. 4, 236 (1958). This paper contains a more complete discussion, with equations, of the star, wagon wheel, and modified wagon wheel designs.

## DISCUSSION

The slotted-tube configuration<sup>1</sup>, as shown in Figure 1, consists of a cylindrical tube of propellant into which has been cast or cut a number of slots. These slots connect the inner and outer surfaces of the tube and extend part of its length.

The configuration offers some striking advantages for the ballistician. Perhaps the most obvious one is its inherent lack of sliver in a non-erosive situation since it is basically an internal-burning cylinder. Because of its simplicity the configuration, with two exceptions, is essentially free from regions of stress concentration such as those which plague the star and other more complex designs. The region at the interior end of each slot is, of course, an exception to that statement; however, our experience has shown this not to be a source of major trouble. The second exception lies in the fact that very thick webs are obtainable in this configuration. In some propellants the stresses arising from the casting and curing of such webs are relieved only by cracking, even though there are no points of stress concentration in the configuration. The design simplicity is also an important factor in mandrel machining and fabrication; the mandrels are much less costly and can be made in a much shorter time than more complicated cores, such as the star and wagon wheel.

Loading fraction increases with increasing web thickness, or burning distance, which permits use of high-burning-rate propellants in highly loaded designs, or of low-burning-rate propellants to obtain very long burning times. In a thick web cylindrical design, the throat area to port area ratio ( $J$ ) would be critical; however, slots make possible loading fractions up to and over 95% with reasonable  $J$  values.

<sup>1</sup>This configuration appears to have been pioneered by the Hercules Powder Company at the Allegany Ballistics Laboratory.

The one apparent disadvantage of the slotted-tube design is the exposure of the motor wall in the slots to the hot, high velocity combustion gases. This condition requires an effective insulating liner, with the requirement becoming more critical with longer burning times.

Some basic assumptions were made about the grain and the manner in which it may be used. It is considered to be case bonded and inhibited at the non-slotted end. Elliptical and hemispherical head and/or tail end filling is not considered; the grain is a right-circular cylinder with slots spaced at equal intervals around the periphery. Although it is thought that the slots will be at the tail end of the grain, they may be placed at the head end at the discretion of the ballistician. The only calculated quantity of concern would be the area of port, which will of course significantly affect the J ratio. It is assumed that burning obeys the normal law and the propellant regresses in parallel layers; erosive burning is ignored. Exact representation of surface and volume is a bit tedious in places, as reference to the equations will indicate. Since the configuration cannot be considered from a two-dimensional standpoint alone, it is necessary to use double integration formulas with some of the small sections of the grain. This may seem unnecessarily burdensome when approximations could be used, and indeed there are indications that these small areas and volumes can be ignored with negligible effect on total values. An attempt has been made to show the derivations in sufficient detail to permit visualization and to adequately describe the sections referred to.

The ballistic quantities of interest are defined similarly to the star design, except that three-dimensional rather than cross-sectional values are used. Thus, the L/D ratio is an important factor because this defines the length of the unit or one-inch diameter grain. Scaling is utilized, as will be noted later.

NOMENCLATURE (Also see Figures 1 and 3)

D	= OD of grain = ID of lined motor
d	= ID of grain
L	= length of grain
l	= length of slot side (to point of tangency with half cylinder at interior end of slot)
N	= number of slots
r	= radius of stress relief cylinder at interior end of slot = half the width of the slot
m	= burning distance for slot burnout = perpendicular distance from point of slot burnout to side of original slot (see Figure 3)
$\beta$	= $\pi/N$
w	= web = $\frac{D-d}{2}$ = burning distance
$S_i$	= initial propellant surface area
$S_f$	= final propellant surface area
$\epsilon$	= volumetric loading fraction
PR	= progressivity ratio = $S_f/S_i$

MATHEMATICAL ANALYSIS

Initial surface is found by calculating the following collection of surfaces: surface of inner perforation, minus surface lost to slots, plus area of the uninhibited end, minus area in end lost to slots, plus area within the slots. Following this order:

$$\begin{aligned} S_i &= \pi d L - N d l \arcsin \frac{2r}{d} - N d \int_0^r \frac{\sqrt{r^2 - y^2}}{\sqrt{\frac{d^2}{2} - y^2}} dy + \frac{\pi}{4} (D^2 - d^2) - 2 N r Z \\ &\quad + \frac{N d^2}{8} \left[ 2 \arcsin \left( \frac{2r}{d} \right) - \frac{4r}{d^2} \sqrt{d^2 - 4r^2} \right] \\ &\quad - \frac{N D^2}{8} \left[ 2 \arcsin \left( \frac{2r}{D} \right) - \frac{4r}{D^2} \sqrt{D^2 - 4r^2} \right] + 2 N l Z + \pi N r Z \end{aligned}$$

$$\begin{aligned}
 & + \left[ \frac{\pi}{2} N dr - 2Nr \int_0^r \sqrt{\frac{x^2 + (\frac{d}{2})^2 - r^2}{r^2 - x^2}} dx \right] - \left[ \frac{\pi}{2} N Dr \right. \\
 & \left. - 2Nr \int_0^r \sqrt{\frac{x^2 + (\frac{D}{2})^2 - r^2}{r^2 - x^2}} dx \right]
 \end{aligned} \tag{1}$$

where  $Z = \frac{1}{2} (\sqrt{D^2 - 4r^2} - \sqrt{d^2 - 4r^2})$ .

If the grain may be considered to have coordinate axes as shown in Figure 2, with the origin at the intersection of the centers of the two cylinders which meet at right angles, the equation of the larger cylinder is

$$x^2 + z^2 = \left(\frac{d^2}{2}\right) \tag{2}$$

while the equation of the smaller cylinder is

$$x^2 + y^2 = r^2. \tag{3}$$

The larger cylinder is the center perforation; the smaller is the rounded end of the slot, actually half of a cylinder. The small areas left over at the intersection of the two cylinders can then be found using the following general formula for the area on a curved surface:

$$\text{Area} = \iint_S \left[ 1 + \left( \frac{\partial z}{\partial x} \right)^2 + \left( \frac{\partial z}{\partial y} \right)^2 \right]^{1/2} dy dx \tag{4}$$

Application of this formula and integration with respect to  $y$  yields the three integrals in  $x$  found in Eq. 1. By suitable transformations the first integral (the third term) becomes

$$A_1 = 2r^2N \int_0^{\frac{\pi}{2}} \frac{\cos^2 \phi d\phi}{\sqrt{1 - k_1^2 \sin^2 \phi}} \tag{5}$$

where  $k_1 = \frac{2r}{d} < 1$ .

This is a complete elliptic integral of the form

$$A_1 = 2Nr^2B(k_1^2)$$

of which  $B(k_1^2)$  is a tabulated function<sup>1</sup>. This integral represents the curved surface on the inner perforation that is displaced by the semi-cylindrical slot end and is subtracted from the surface of the inner perforation.

The major part of the surface inside the semi-cylindrical slot end is found by considering a right circular half-cylinder from the outer propellant surface to the inner perforation parallel to the Z-axis (Figure 2). The second integral of the  $S_i$  equation, along with the preceding term in the same equation, deals with the surface around the side of the small cylinder below the plane normal to the Z-axis at the intersection of the inner perforation with the Z-axis. This surface is added. The last integral and its preceding term are analogous but at the outer surface of the grain, and this area is subtracted.

The latter two integrals can also be transformed into complete elliptic integrals; however, because they are largely cancellative and are relatively small it was decided that their effect would be negligible and so they are omitted from actual calculations.

In considering final surface a new problem presents itself. In some cases the web will burn out before the slots burn through the "wall" separating them. In other cases, where the slots are closer together and/or the web thicker, the slots may "join" before web burnout so that final surface will be limited entirely to the unslotted portion of the grain. However, since burning also occurs in the end of the slot, progressing toward the unslotted end of the grain, a scalloped effect will be noted on the final surface as viewed perpendicular to the Y-axis (see Figure 4).

<sup>1</sup>E. Jahnke and F. Emde, "Tables of Functions", 4th ed., Dover, New York (1945), p. 82.

Since different equations will be required in the two cases just described, it is well to define a condition that specifies which situation exists for the particular grain under consideration. From Figure 3 it may be seen that

$$m = \frac{D}{2} \sin \beta - r \quad (6)$$

If  $m = w$ , the sides of the slots meet at the motor wall at web burnout. If  $m > w$ , they will not meet before web burnout; but if  $m < w$ , they will intersect to give the scalloped effect mentioned above and shown in Figure 4.

In the cases where  $m \geq w$ , the following formula for final surface will suffice:

$$\begin{aligned} S_f &= w \left[ \pi D - ND \arcsin \frac{2(r+w)}{D} \right] + \pi D - 2N(r+w)^2 B(k_2^2) + \pi D L \\ &= \pi D(L-w) - ND(l-w) \arcsin \frac{2(r+w)}{D} - 2N(r+w)^2 B(k_2^2) \end{aligned} \quad (7)$$

$$\text{where } k_2 = \frac{2(r+w)}{D} < 1.$$

The function  $B(k_2^2)$  is analogous to  $B(k_1^2)$  which was obtained from Eq. 5 and the same tabulation is used for its evaluation.

Final surface in the case  $m < w$  is given by Eq. 8.

$$\begin{aligned} S_f &= \pi D \left[ L - (l + r + w) \right] + 2N \int_0^{\frac{D}{2} \sin \beta} \int_{\sqrt{(r+w)^2 - x^2}}^{r+w} \\ &\quad \left[ 1 + \left( \frac{-x}{(\frac{D}{2})^2 - x^2} \right)^2 \right]^{1/2} dy dx \end{aligned} \quad (8)$$

The double integral represents the scalloped part of the shaded area in Figure 4. Integration with respect to  $y$  transforms Eq. 8 into Eq. 9.

$$S_f = \pi D \left[ L - (l + r + w) \right] + \pi D (r + w)$$

$$- ND \int_0^{\frac{D}{2} \sin \beta} \frac{\sqrt{(r+w)^2 - x^2}}{\sqrt{(\frac{D}{2})^2 - x^2}} dx \quad (9)$$

The integral (including the factor  $ND$ ) reduces to the difference of incomplete elliptic integrals of the first and second kind. By suitable transformations it can be put into the form

$$I = 2N (r+w)^2 \int_0^\phi \frac{\cos^2 \psi d\psi}{\sqrt{1 - k_3^2 \sin^2 \psi}}$$

$$= 2N (r+w)^2 \int_0^\phi \frac{(\sqrt{1 - \sin^2 \psi})^2}{\sqrt{1 - k_3^2 \sin^2 \psi}} d\psi \quad (10)$$

which becomes

$$I = 2N (r+w)^2 \left[ \int_0^\phi \frac{d\psi}{\sqrt{1 - k_3^2 \sin^2 \psi}} - \int_0^\phi \frac{\sin^2 \psi d\psi}{\sqrt{1 - k_3^2 \sin^2 \psi}} \right] \quad (11)$$

where  $\phi = \arcsin \frac{\frac{D}{2} \sin \beta}{r+w}$

$$\text{and } k_3 = \frac{2(r+w)}{D} = k_2$$

Legendre's standard form of the elliptic integral of the first kind is

$$F(k, \phi) = \int_0^\phi \frac{d\psi}{\sqrt{1 - k^2 \sin^2 \psi}} \quad (12)$$

and of the second kind is

$$E(k, \phi) = \int_0^\phi \sqrt{1 - k^2 \sin^2 \psi} \quad d\psi \quad (13)$$

If Eq. 13 is rewritten as

$$\begin{aligned} E(k, \phi) &= \int_0^\phi \frac{(\sqrt{1 - k^2 \sin^2 \psi})^2}{\sqrt{1 - k^2 \sin^2 \psi}} \quad d\psi \\ &= \int_0^\phi \frac{d\psi}{\sqrt{1 - k^2 \sin^2 \psi}} - k^2 \int_0^\phi \frac{\sin^2 \psi \quad d\psi}{\sqrt{1 - k^2 \sin^2 \psi}} \end{aligned} \quad (14)$$

then

$$\int_0^\phi \frac{\sin^2 \psi \quad d\psi}{\sqrt{1 - k^2 \sin^2 \psi}} = \frac{F - E}{k^2} \quad (15)$$

Therefore, Eq. 9 can be reduced to the form

$$S_f = \pi D (L - l) - 2N (r + w)^2 \left[ F - \frac{F - E}{k^2} \right] \quad (16)$$

The functions  $F(a, \phi)$  and  $E(a, \phi)$ , where  $k = a$ , are tabulated<sup>1</sup>

---

<sup>1</sup>Ibid, pp 62-72

Because it is theoretically non-existent, no equation is required for sliver.

The volumetric loading fraction is given by the following equation:

$$\begin{aligned}\epsilon &= \frac{\text{volume of propellant}}{\text{volume of motor}} \\ &= \frac{4}{\pi D^2 L} \left[ \frac{\pi}{4} L (D^2 - d^2) - r l N (\sqrt{D^2 - 4r^2} - \sqrt{d^2 - 4r^2}) \right. \\ &\quad + \frac{d^2 l N}{8} \left( 2 \arcsin \frac{2r}{d} - \frac{4r}{d^2} \sqrt{d^2 - 4r^2} \right) \\ &\quad - \frac{D^2 l N}{8} \left( 2 \arcsin \frac{2r}{D} - \frac{4r}{D^2} \sqrt{D^2 - 4r^2} \right) \\ &\quad \left. - \frac{\pi}{4} N r^2 (\sqrt{D^2 - 4r^2} - \sqrt{d^2 - 4r^2}) \right] \quad (17)\end{aligned}$$

In this equation the small volumes analogous to the surfaces represented by elliptic integrals have been ignored. As in the case of the surfaces, they are largely cancellative, and the labor involved in obtaining the equations and hence the numerical values appear to be very much out of proportion to their effect on the whole value for loading fraction.

It is usually desirable, if not necessary, for the rocket grain designer to know the shape of the pressure-time curve which will be produced by his grain. Essential to this is the ability to calculate the propellant surface area as a function of the distance burned normal to the surface.

The burning surface of a slotted-tube grain may pass through three distinct phases during the course of its consumption. Initially the propellant will burn outward in the interior cylinder, and sideways and lengthwise in the slots. If the web is thick enough and the slots close enough together, eventually the curved cylindrical interior surface separating adjacent slots will disappear into a line contact between the two slots. This is pictured in cross section in Figure 3, and it may be seen that this occurs when  $x = x^*$ , which is defined as

$$x^* = \frac{d \sin \beta - 2r}{2(1 - \sin \beta)} \quad (18)$$

As  $x$  increases further, the propellant between the adjacent slots diminishes rapidly and will vanish before  $x = w$ . Thus the third phase of burning involves only the unslotted, cylindrical section of the grain. This section is inhibited on one end but burns on the other end which now has a scalloped appearance.

When  $x > x^*$ , the distance  $Z_x$  (see Figure 3 again) must be calculated by a different formula than when  $x < x^*$ . An additional complication occurs when the slot length is less than web, permitting the end-burning effect to extend into the region characterized by the semi-cylindrical slot ends. Equations are given which, in the interest of practicality, approximate to sufficient accuracy the surface changes required when  $l < w$ . The equations for all cases are as follows:

CASE IA:  $x < x^*, x \leq l$

$$S_x = \pi (d + 2x) (L - x) + \frac{\pi}{4} \left[ D^2 - (d + 2x)^2 \right] - 2N (r + x)^2 B(k_x^{-2})$$
$$+ \frac{N}{4} (d + 2x) (d + 6x - 4l) \arcsin \frac{2(r + x)}{d + 2x}$$

$$+ 2N (\ell + 1.070796 r + 0.070796 x) Z_x$$

$$- \frac{ND^2}{4} \arcsin \frac{2(r+x)}{D} \quad (19)$$

$$\text{where } k_x = \frac{2(r+x)}{d+2x} < 1$$

$$\text{and } Z_x = \frac{1}{2} \left( \sqrt{D^2 - 4(r+x)^2} - \sqrt{(d+2x)^2 - 4(r+x)^2} \right)$$

CASE IB:  $x < x^*, x \leq m, x > \ell$

$$\begin{aligned} S_x = & \pi (d+2x) (L-\ell) + \frac{\pi}{4} \left[ D^2 - (d+2x)^2 \right] + 2N (r+x) \left( \frac{\pi}{2} - \zeta \right. \\ & \left. - \cos \zeta \right) Z_x - \left[ \pi (d+2x) (r+w) \right] \left[ \frac{\frac{\pi}{4} (r+x)^2 + (r+m) (x-\ell)}{(r+x) (r+m)} \right. \\ & \left. - \frac{\frac{1}{2} (r+x) (\cos \zeta) (x-\ell) + \frac{1}{2} (r+x)^2 \zeta}{(r+x) (r+m)} \right] \end{aligned} \quad (20)$$

$$\text{where } \zeta = \arcsin \frac{x-\ell}{r+x}$$

$Z_x$  is the same as in Eq. 19

$$\text{and } m = \frac{D}{2} \sin \beta - r$$

CASE IIA:  $x \geq x^*, x \leq m, x \leq \ell$

$$S_x = \pi (d+2x) (L-\ell) + 2NZ_x (\ell-x) + \frac{NZ_x^2}{2} \sin 2\beta$$

$$+ \frac{ND^2}{8} (\lambda_x - \sin \lambda_x) + \pi N (r+x) Z_x - 2N (r+x)^2 B(k_x^2) \quad (21)$$

$$\text{where } Z_x = \frac{1}{2} \sqrt{D^2 - 4(r+x)^2} - \frac{r+x}{\tan \beta}$$

$$\lambda_x = 2 \left[ \beta - \arcsin \frac{2(r+x)}{D} \right]$$

$$\text{and } k_x = \frac{2(r+x)}{d+2x} < 1$$

**CASE IIB:**  $x \geq x^*, x \leq m, x > l$

Use Eq. 20 (Case IB).

**CASE III:**  $x > x^*, x > m$

$$S_x = \pi (d+2x) (L-l) - 2N (r+x)^2 \left[ F_x - \frac{F_x - E_x}{k_x^2} \right] \quad (22)$$

$$\text{where } k_x = \frac{2(r+x)}{d+2x} < 1$$

$F_x$  and  $E_x$  are functions of  $\alpha$  and  $\phi$ ,

where  $\alpha = \arcsin k_x$

and  $\phi = \arcsin \frac{(d+2x) \sin \beta}{2(r+x)}$

### CALCULATION AND PRESENTATION OF DATA

The equations listed in the previous section, which describe the interrelationship of the design parameters, have been programmed for the Royal Precision LIP-30 Computer, a small, digital electronic computer. Quantities designated to be varied over a fairly wide range were progressivity ratio, web, grain length, and number of slots. With those quantities specified, the computer determined  $\ell$ , the slot length, and then calculated the initial and final surfaces, the volume and loading fraction, and the port area.

All calculations were made for  $D = 1.0$ , so that  $L$  is actually equivalent to the  $L/D$  ratio. Scaling is accomplished by multiplying all linear dimensions,  $d$ ,  $w$ ,  $\ell$ ,  $L$ , and  $r$  by the desired diameter; by multiplying propellant surface areas and grain port area by the diameter squared; and by multiplying volume by the diameter cubed. Progressivity ratio and loading fraction are, of course, independent of diameter.

The radius  $r$ , essentially a stress relief fillet, was chosen to be  $0.03D$ , the same value that was used in earlier star design work. No difficulty has been experienced in using this value in a number of slotted-tube grains.

In order that the results of the computer program be made generally available and more easily used, it was decided to exhibit on graphs as many of the data as possible. Accordingly, the graphs which are reproduced in this report were prepared. There are eighty-three graphs covering the range of  $N$ 's from two through five and of  $L/D$  ratios from one through fifteen. Length to diameter ratios of less than one were calculated; however, analysis of the results led to the conclusion that they would be of little or no value. Grains which are that short will surely require head and/or tail filling and an inhibitor arrangement different from that proposed here; the graphs could not be extrapolated to cover these possibilities.

From the graphs one can obtain information relating  $N$ ,  $L$ ,  $\ell$ ,  $\epsilon$ ,  $PR$ ,  $w$ , and  $S_i$ . Also of course  $S_f$  can be found from  $S_i$  and  $PR$ . There are two sets of web lines: the wider lines with the arrow heads pointing down relate  $w$ ,  $\epsilon$ ,  $\ell$ , and  $PR$ . The narrower lines with arrow heads pointing up relate  $w$ ,  $\ell$ , and  $S_i$ .

In using the graphs, one might have specified the web (or loading fraction), the progressivity ratio and the  $L/D$  ratio. After deciding upon the number of slots to be used, reference to the proper wide web lines will show the slot length required. Relating that slot length to the corresponding narrow web line will show the initial surface of the design.

An important piece of information that could not be included on these design graphs is the shape of the surface-time trace. The characteristic shape of the trace of a slotted-tube grain is initially progressive, then it rounds over smoothly and decreases until web burns out or the slots burn through, whichever occurs first. In those designs where there are enough slots and the web is thick enough ( $w > m$ , see Table I) so that the slotted end is consumed before web burnout, the final portion of the trace will again become progressive. In short  $L/D$  motors, say  $L/D = 2$ , the effect of burning the scalloped end left by the slots will pretty well neutralize the progressive tendency of the cylindrical portion of the grain.

Table I  
Values of  $m$

<u>N</u>	<u>m</u>
2	> radius
3	0.4030
4	0.3235
5	0.2638

Something can be done, however, to give the ballistian some idea of the severity of the "hump" in the surface-time trace without solving the equations for surface as a function of distance burned.

In Figure 5a the maximum height of the hump as a percent of initial surface is plotted as a function of web, with  $L/D$  as a parameter, PR constant at 1.00 and  $N = 2$ . The following example will perhaps illustrate how the data on this graph may be extrapolated to other PR values.

Assume  $L/D = 10$ ,  $w = 0.40$  and PR = 1.10. From Figure 5a it is seen that the "hump factor" for PR = 1.00 is 111.5, meaning that the maximum surface is 11.5% greater than initial surface. This occurs near the midpoint of web. In the problem at hand, if surface increased monotonically to a value 10% greater than  $S_i$ , i.e., PR = 1.10, then at the midpoint of web the surface would be 5% greater than  $S_i$ . Thus, adding to this value the 11.5% obtained from the graph a "hump factor" of 116.5 is obtained. By the same token, a design with a PR = 0.90 would have a hump factor of 106.5, and for PR = 0.80 the factor would be 101.5. These values are almost exactly those calculated from the  $S_x$  equations.

From Figures 5b, 5c, and 5d it is seen that the situation is a little different for  $N > 2$  because in thick web designs there is a region of minimum surface when the slots burn through. Accordingly, there will be a hump in the early portion of the surface-time trace (at about  $\frac{m}{2}$ ), and a dip in the trace (at m) followed by a progressive rise to web burn out. It is believed that these graphs will be useful in guiding the designer, although he may wish to calculate exactly the surface-time history of the design finally chosen.

#### APPLICATION

Perhaps a brief word is in order concerning the use of this work by Rohm & Haas Company. Ten slotted-tube designs have been made for use in test motors. These have loading fractions ranging from 46% to 95.5% and have been used in motors from 2-inches to 23-inches in diameter. The design has lived up to its expectations and the problem of insulation in the slots has not been too difficult in the motors used.

Certainly, as burning times are increased, the problem will increase in severity and better liners will be required. A 23-inch diameter motor containing a thousand pounds of propellant has been fired successfully.

An example of a pressure-time trace obtained from the static firing of a slotted-tube configuration is shown in Figure 6, the solid line. Inasmuch as this motor had a hemispherical head end, the trace is more regressive than indicated by the theoretical surface-time trace for the cylindrical portion of the grain (Figure 6 dotted line). When the additional surface area in the head end, and the decrease in length of the grain from this effect is included, the theoretical trace is as shown by the dashed line in Figure 6. The propellant used had a pressure exponent of 0.55.

This particular design has three slots, a web of 0.184 D,  $L/D = 5.66$ ,  $\ell = 2.40 D$ ,  $\epsilon = 58.3\%$ ,  $PR = 1.01$  (right circular cylinder), area of port of  $0.349 D^2$ , and  $S_i = 14.706 D^2$  (including head end). The actual motor size was  $6 \times 33$  inches and the J value for this particular shot was 0.214. The ratio of the pressure integral during burning time to the total pressure integral was 0.967, comparable to that obtained with purely cylindrical grains under non-erosive conditions. The regressivity exhibited in the firing was probably caused by the differential in burning rates between the head and tail as the result of pressure drop along the grain length.

#### ACKNOWLEDGEMENTS

The author wishes to express his appreciation to Mrs. Mary Lou Cagle for invaluable assistance in running off the calculations on the computer and for plotting all the graphs, to Mrs. Ann Locke, Mrs. Eunice Shelton and Miss Marie Smith for assistance in preparing the design graphs, and to Mr. Howard Wilson for locating an error in the mathematical work.

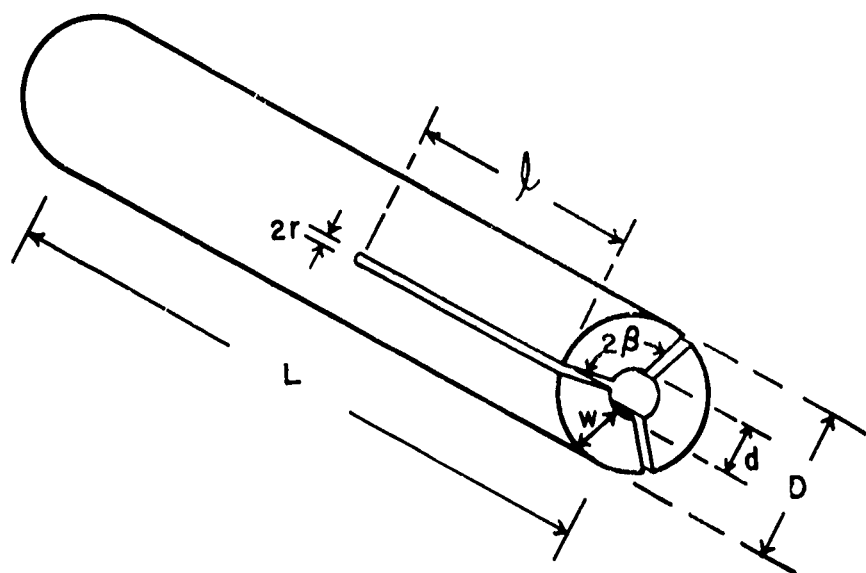


Fig. 1 The slotted-tube configuration

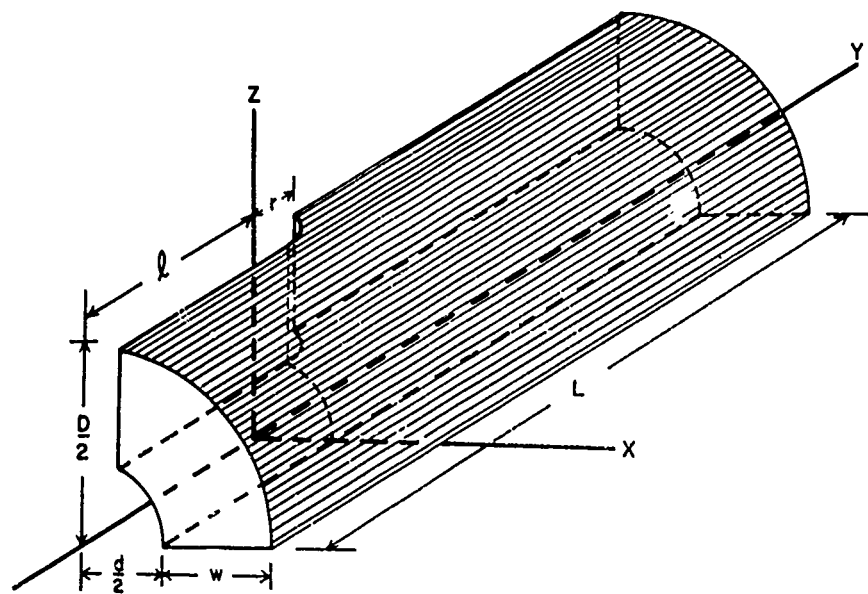


Fig. 2 Sector of slotted-tube configuration showing location of coordinate axes

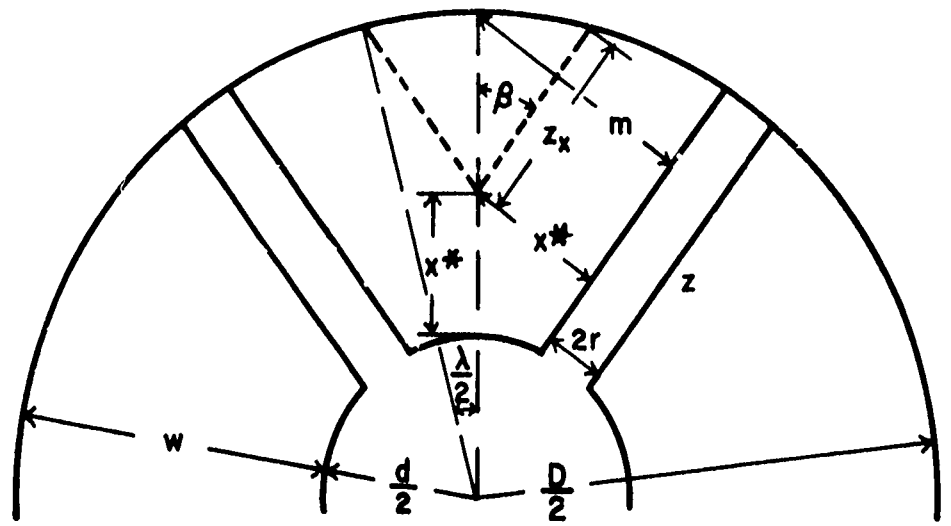


Fig. 3 Cross section of slotted - tube configuration

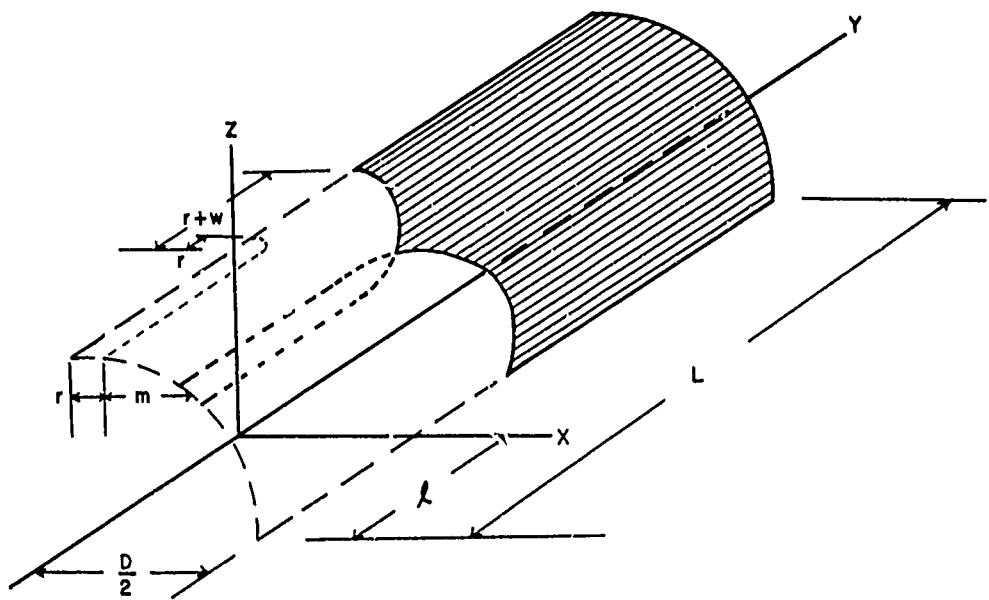
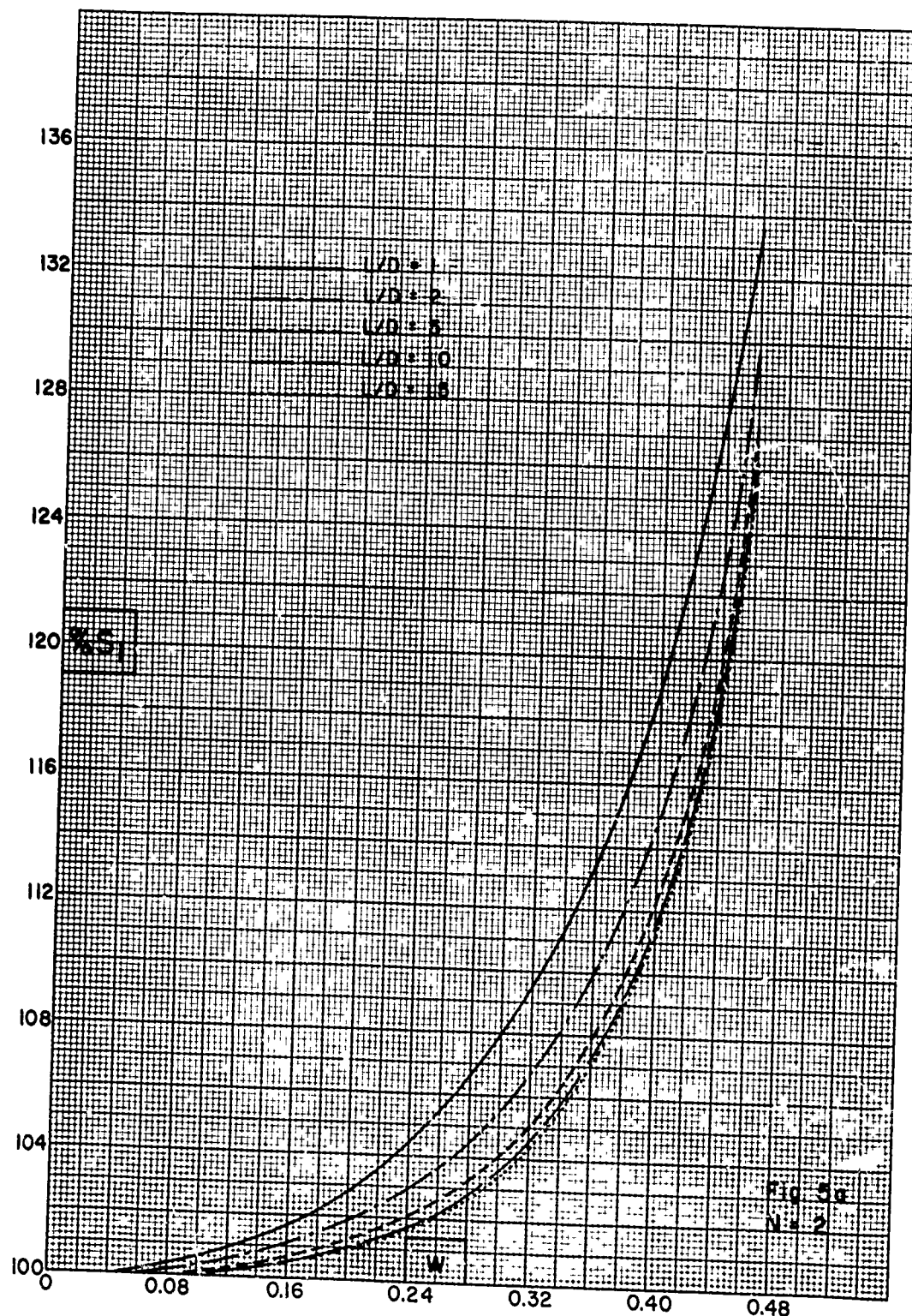
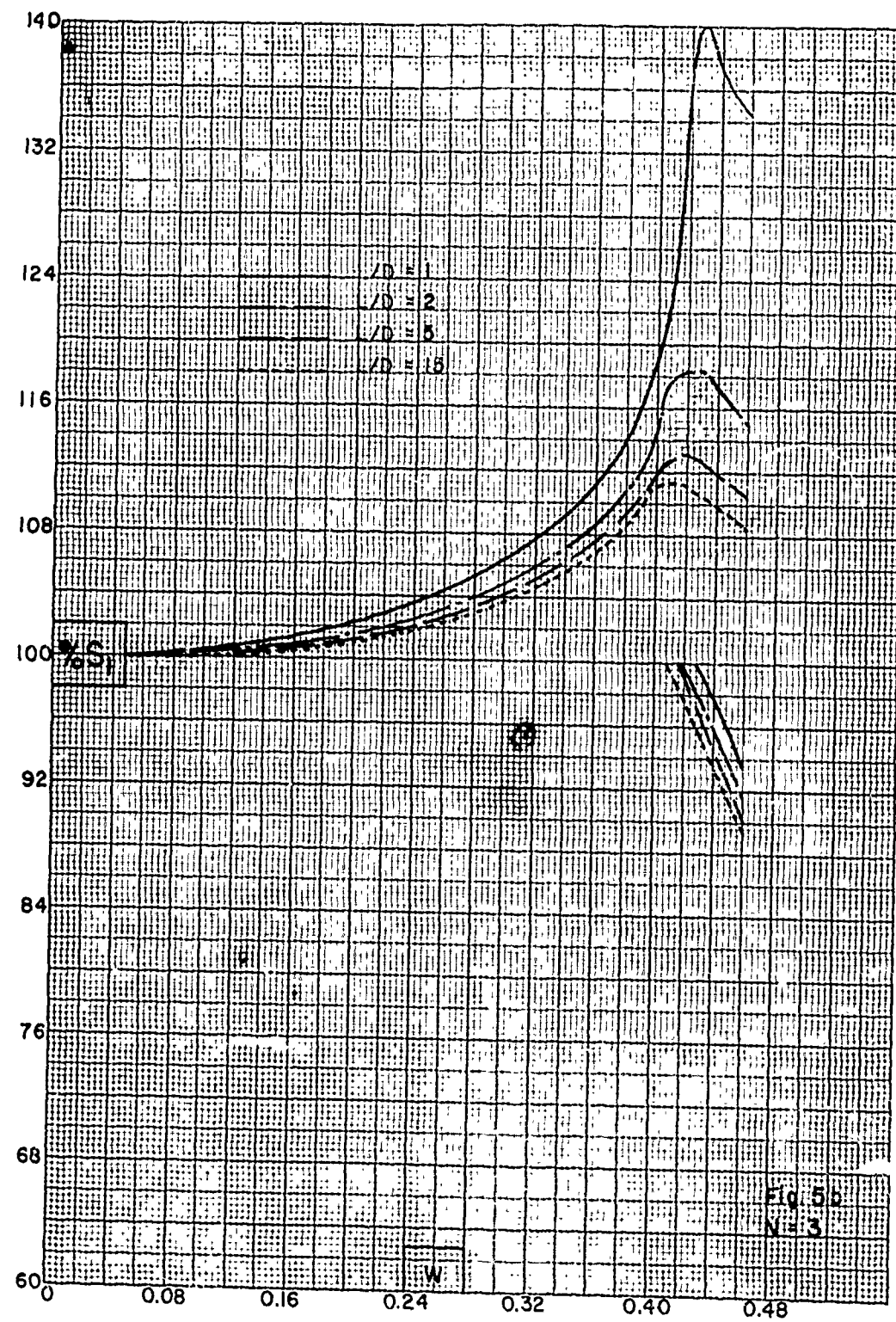
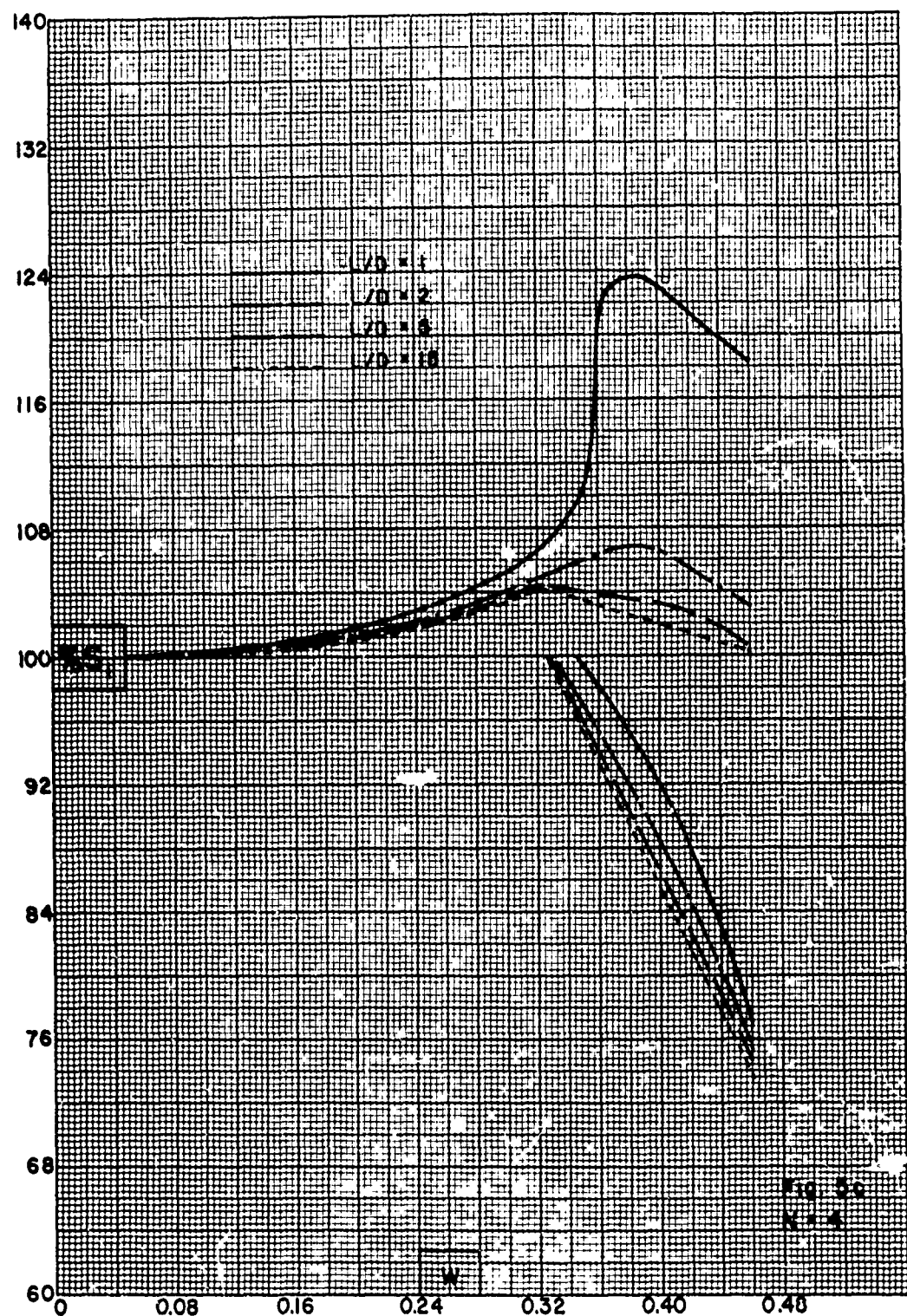
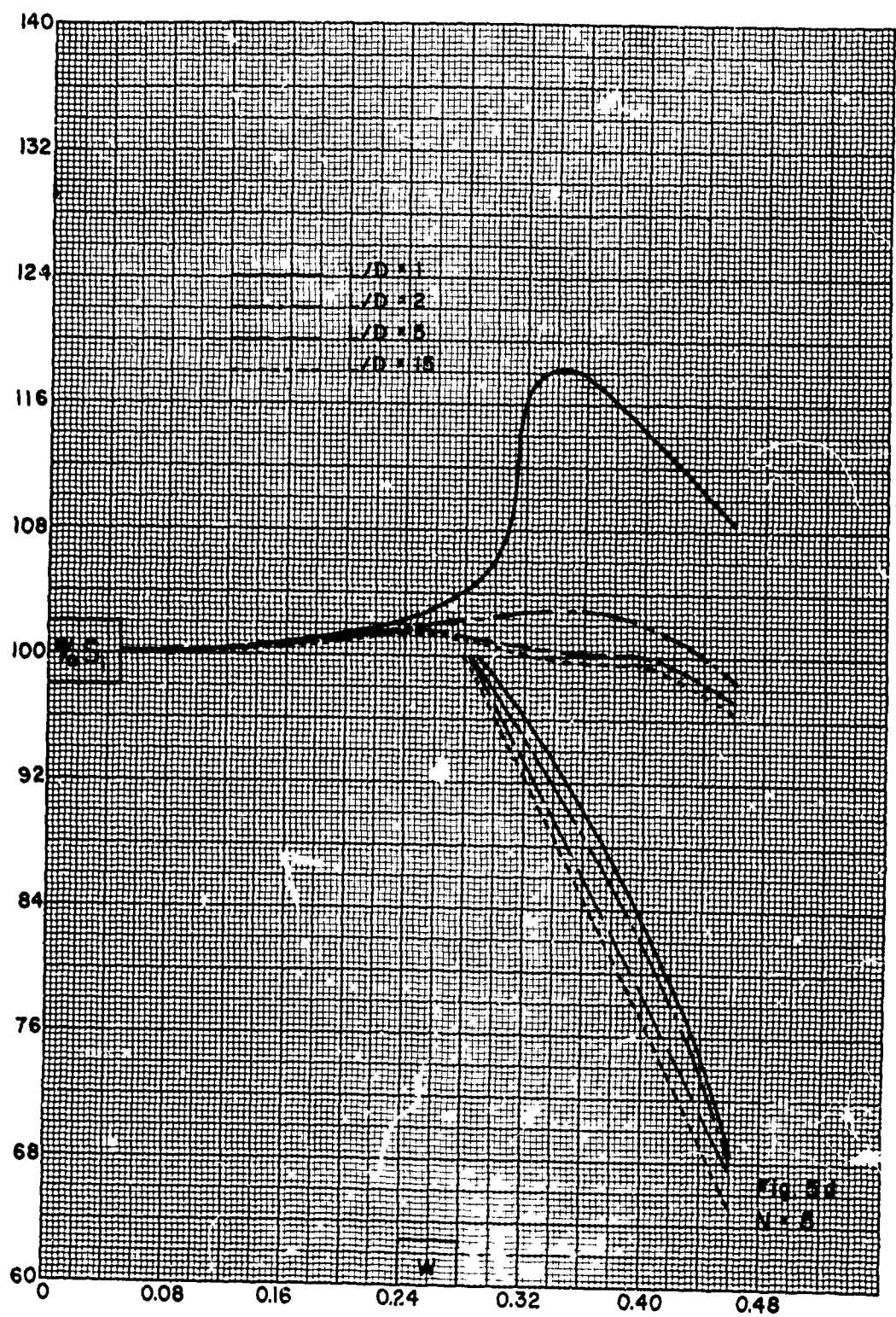


Fig. 4 Final surface when  $m < w$









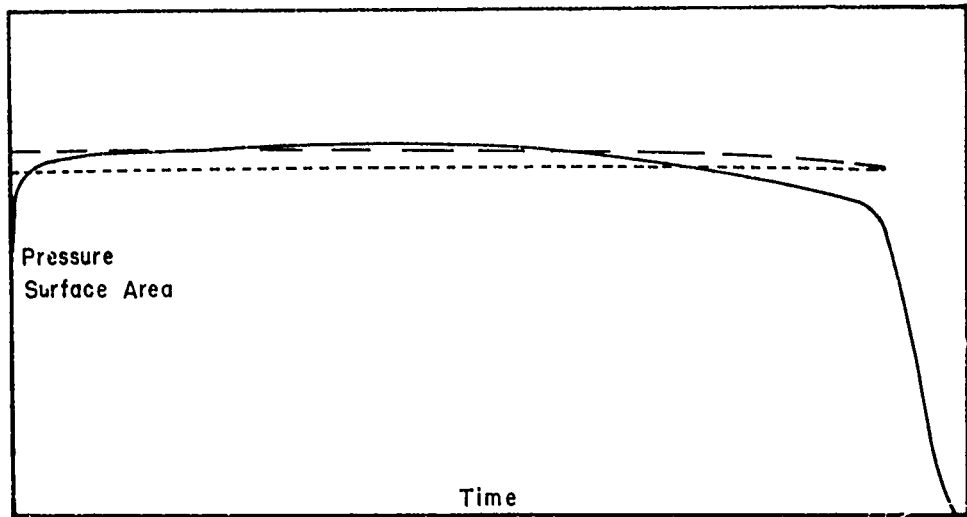


Fig. 6 Surface-time and pressure-time traces for a slotted-tube design.

